Experimental assessment of a PCM to air heat exchanger for heating peak loads shaving

Matthieu Labat, Joseph Virgone, Damien David, Frédéric Kuznik

Experimental assessment of a PCM to air heat exchanger for heating peak loads shaving

Labat M.*,, Virgone J. *,**, David D. *,**, Kuznik F*,****

* Université de Lyon, 69361 Lyon Cedex 07, France
**CETHIL UMR5008, INSA-Lyon, Université Lyon1, 69621 Villeurbanne Cedex, France

E-mail: matthieu.labat@insa-lyon.fr

Keywords: Phase Change Material, heat storage, experimental tests

1. INTRODUCTION

Nowadays, thermal energy storage systems (TESS) are essential to rationalize the energy management and the use of environmental energy potential. Concepts including phase change material (PCM) are technically mature for building applications and innovations. Among the existing concepts of TESS, PCM to air heat exchanger can directly be integrated in building ventilation systems in order to store energy for heating peak loads shaving [1]. A similar system could also be used for cooling purposes, as presented in [2]. Here, during the off-peak period, the air is heated by a heat pump and passes through the heat exchanger to store energy. This energy is released during the peak period to heat the building and reduce the required heating load. The objective is to stop the heat pump without affecting the thermal indoor comfort. Quantitatively, the heat exchanger is designed so it can replace about a 1 kW heating system during 2 hours.

The second issue of this work is to provide detailed results suitable with the validation of numerical models. On this subject, data from several experiments are collected and presented in [3] and the authors are underlining the lack of data. For this reason, the geometry of the exchanger will be detailed here and the uncertainty associated with the heating power measurement will be given.

In this paper, the design and the instrumentation of the heat exchanger is first presented. Next, the tests simulating a ventilation system, and realized in our laboratory setup, are presented and discussed. In the conclusions, design guidelines are given in order to meet the storage unit specification requirements.

2. EXPERIMENTAL FACILITY

The heat exchanger was designed so it contains almost 30 kg of PCM. First, the PCM properties will be presented. Then, a short description of the heat exchanger and of the air supply system will be given. Finally, this section will focus on the instrumentation.

2.1 PCM properties

The selected material is paraffin based. Its commercial name is Microtek 37D[1] and its thermal properties were measured in laboratory (EDF - R&D). Results are presented in Table 1.

Precisely, the melting heat is measured on a 0.40505 g sample, using the DSC method (Differential Scanning Calorimertry) at a 0.15°C.min^{-1} heating rate. Phase change is observed when the temperature is growing from 30 to 38°C and a temperature peak is observed at 37.2°C. The same method is applied to measure the solidification heat and a very good agreement is obtained with the measured melting heat (0.1 %). However, the temperature peak is different (31.7°C).

Table 1: Thermal properties of the material

	Solid state	Liquid state
Density (kg.m^{-3})	870	779
Thermal conductivity (W.m^{-1}.K^{-1})	0.24	0.18
Heat capacity (kJ.kg^{-1}.K^{-1})	2,360 (20°C)	2.453 (45°C)
Melting heat (kJ.kg^{-1}.K^{-1})	230	

2.2 Design of the PCM containers

The PCM is distributed into 34 plane-parallel aluminium containers (dimensions: 0.018 m × 0.200 m × 1.000 m). Each container is made of two identical cavities which are filled with PCM. Each cavity is sealed with aluminium sidings (0.016 m × 0.016 m × 0.048 m) and silicon.

However, the melting of PCM results in density change (see Table 1). To prevent PCM leakages, the cavities are partially filled and air vents (achieved by the simple mean of copper tubes) are placed at the top of the aluminium sides as presented in Figure 1.

During the experiments, no mass losses have been identified. The total mass of empty containers is 18.53 kg, and the total mass of PCM is 27.88 kg.

[1] http://www.microteklabs.com/pdfs/MPCM-37D%20Product%20Data%20Sheet.pdf

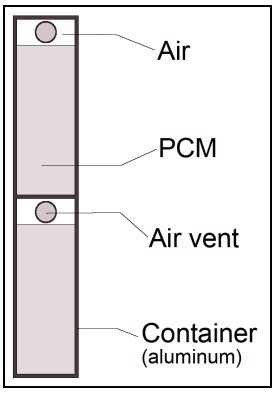

Figure 1: Scheme of a single container filled with PCM

2.3 Design of the heat exchanger

The heat exchanger is made of the 34 containers and cooling fins (the total mass of the cooling fins is 4.69 kg). Containers are pilled up by two, which results in 17 blocks (0.400 m × 0.018 m × 1.000 m). The blocks are separated by fins of identical cross-section (see Figure 2). The fins are designed so that the air layer which is separating two blocks is split into 50 channels (0.080 m × 0.018 m × 1.000 m).

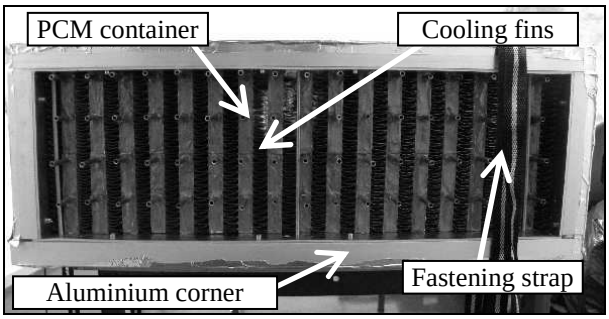

Figure 2 : Picture of the front of the heat exchanger

The whole assembly is surrounded with aluminium plates and the overall cross-section is 0.200 m × 0.630 m. These aluminium plates are maintained together with aluminium rails, screws and nuts, located on the external side of the heat exchanger. Finally, the exchanger is insulated using a 0.04 m thick layer of polystyrene and mineral wool.

2.4 Setting the heat exchanger in the air-supply system

The heat exchanger is placed into a closed-loop wind tunnel (the exhaust air is recycled). The air supply system includes a complete HVAC system (Heating, Ventilation Air Conditioning) and a 2.50 m long testing section within its upper part.

The exchanger is placed in the test section as presented in Figure 3. However, its cross-section is smaller than the one of the air inlet (1.00 m × 1.00 m). In order to control the airflow rate crossing the exchanger, both an upstream and a downstream section are added.

The whole system is designed in order to be as airtight as possible. For example, fastening techniques are preferred to drilling techniques to gather the different part of the system. Moreover, each juncture is sealed with aluminium tape.

The upstream section is made of two parts. In the first one, the cross-section is gradually reduced to the targeted cross-section (slope: 30°). In the second part, the cross-section remains constant so that the airflow can stabilize. The overall length of the upstream section is 1.000 m.

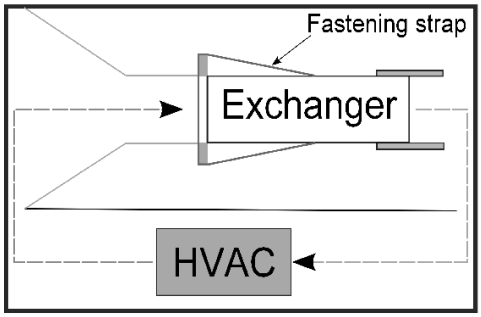

Figure 3: Scheme of the air supply system

To limit air leakage, the exchanger has to be tightened on the downstream section. This can be achieved by adding 0.030 m wide aluminium corners at the edges of the heat exchanger (see Figure 2). Next, a rubber strip with identical dimensions is screwed on these corners (not visible in Figure 2). Finally, two fastening straps are passing through the aluminium rails (the ones which are maintaining the aluminium plates altogether). These straps are wrapped around the downstream section and stretched (see Figure 3).

The upstream section is much simple. It is a 0.400 m long constant cross-section element. Its cross-section is slightly greater than the one of the heat exchanger. The air-tightness is achieved by the mean of a plastic foil maintained with aluminium tape. Finally, polystyrene elements are added inside in order to extend the cross-section homogeneously. A picture of the heat exchanger installed in the testing section of the air-supply system is given in Figure 4.

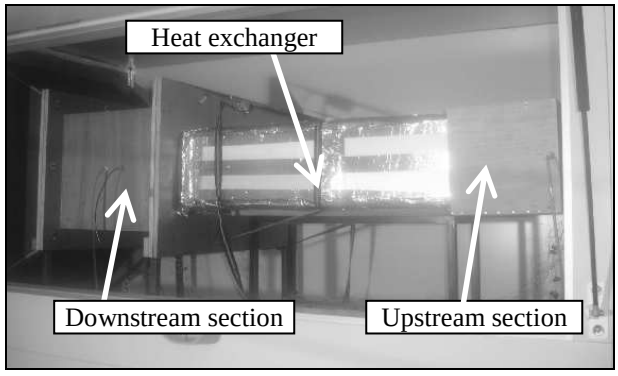

Figure 4: Picture of exchanger installed in the air-supply system

2.5 Instrumentation

The instrumentation is selected in order to estimate the heating power, which can be calculated with equation (1):

$$P = \rho_A(T) \cdot \dot{Q}_V \cdot C_{P,A} \cdot (\Delta T_A) \qquad (1)$$

Where: P is the heating power (W);
ρ_A is the air density (kg.m^{-3});
Q_V is the airflow rate (m^3.s^{-1});
$C_{P,A}$ is the heat capacity of air (= 1004 J.kg^{-1}.K^{-1});

ΔT_A is the temperature difference between the inlet and the outlet sections of the heat exchanger (K).

ρ_A can be estimated with equation (2):

$$\rho_A = 1.293 \cdot \frac{273.15}{T_A(K)} \quad (2)$$

Therefore, it is necessary to give precise estimations of both the airflow rate and ΔT_A. The airflow rate is monitored by the air-supply system. Because of air leakages however, the airflow rate crossing the heat exchanger might be smaller and still have to be estimated. For this reason, a unidirectional hot wire anemometer is set inside the downstream section. It is sensitive to air speeds ranging from 0.05 to 2.50 m.s^{-1} and is 4 % but not to the airflow direction.

To estimate the temperature difference, 5 differential thermocouples are installed, both in the upstream and downstream sections. They are placed in cross-sections located 0.15 m away from the heat exchanger and fixed on nylon ropes as presented in Figure 5. One sensor is located in the middle of the cross section, while four others are located 0.05 m away from the walls. These thermocouples were all calibrated in laboratory, which allows achieving 0.3°C accurate measurements. Three classical T-type thermocouples are added at these locations (middle, top and right positions) and measure the air temperature.

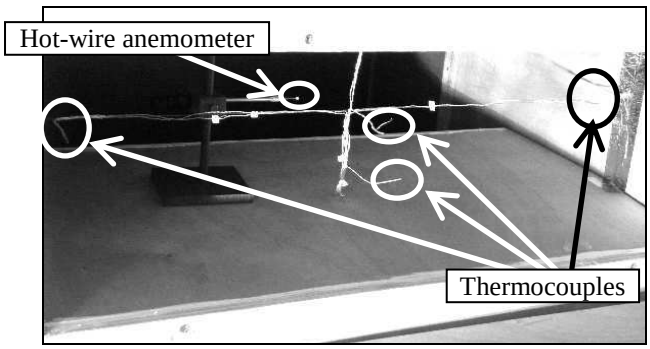

Figure 5: Picture of the sensors installed in the downstream section

This system will be integrated in an air distribution system. The induced pressure difference is then a major issue and has to be estimated. Here, a pressure difference device is connected both to the upstream and the downstream sections, close to the position of the temperature sensors (not visible in Figure 4). It is installed so it measures the static pressure.

Finally, more than thirty thermocouples are used to measure temperatures at various locations inside the heat exchanger. For the sake of clarity, only a few will be presented and discussed in this paper. Later, temperature measurements achieved in the container located in the middle of the heat exchanger will be presented. There are three thermocouples installed in the middle of the cavities filled with PCM; two are positioned 0.05 m away from the edges and the third one is located at middle-length.

The number and accuracy of the sensors are summarized in Table 2.

Table 2: Description of the instrumentation

Physical parameter	Number	Accuracy
Temperature difference (°C)	5	± 0.3°C
Air velocity (m.s^{-1})	1	± 0.08 m.s^{-1}
Pressure difference (Pa)	1	± 0.5 %
Temperature (°C)	32	± 0.5°C

3. RESULTS AND DISCUSSION

The airflow rate is set to 900 m^3.h^{-1} during the whole experiment. The objective is to observe the complete MCP melting and solidification cycle. The inlet air temperature evolution is composed of two (20 and 45°C) over 4 hours. In this chapter, both temperature and airflow measurements will be presented. Finally, the heat power and the cumulative energy will be estimated and discussed.

3.1 Temperature measurements

The MCP temperature measurements achieved during the melting and the solidification periods are presented in Figure 6 and in Figure 7 respectively. The time reference (t =0 h) corresponds to the temperature change. The air temperature at the inlet is the average value of the three measurements achieved in the downstream section.

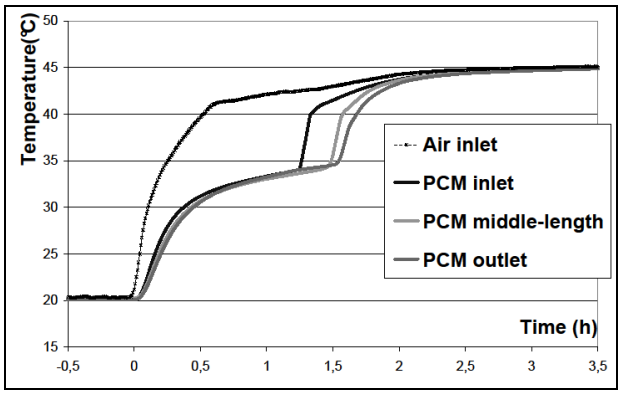

Figure 6: Temperature measurements during the melting period

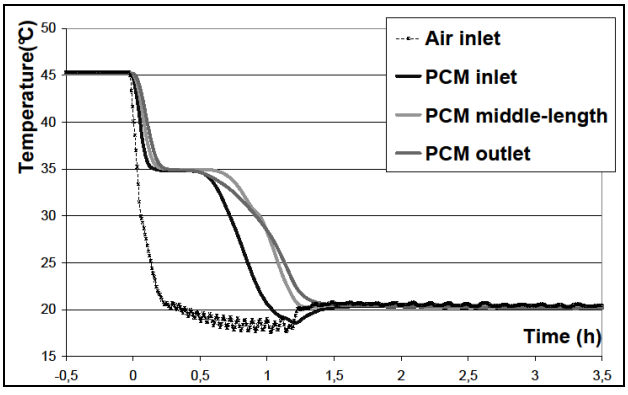

Figure 7: Temperature measurements during the solidification period

First, the temperature increase at the inlet is not immediate; during the heat storage period, the inlet temperature reaches 40°C

almost 30 minutes after the beginning of the temperature change. It is faster for the temperature change from 45 to 20°C (18 minutes), yet a lower temperature is measured and ± 0.6°C variations are observed. This is probably due to the air-supply controlling system, which was calibrated when the testing section was empty. As this calibration was not achieved at the laboratory, it can be hardly modified and this assumption can not be verified. Still, temperature measurements achieved directly in the PCM are showing a regular behaviour. Heating rates are calculated for different temperature ranges and presented in Table 3.

Table 3: Measured heating rate during the melting and solidification periods for typical temperature ranges.

Period	Temperature range °C	Heating rate °C.min^{-1}
Heat storage	[20 ; 30]	0.44
	[30 ; 35]	0.037
	[35 ; 40]	0.93
Heat release	[45 ; 40]	0.91
	[30 ; 25]	0.60

During the heat storage (see Figure 6), the temperature increases slowly from 30 to 34°C (the heating rate is approximately 0.037°C.min^{-1}), which corresponds to the melting of the material. During this period, temperature is 1°C homogeneous within the PCM, which corresponds to the uncertainty range. When the PCM is melted, temperature increases quickly to meet the inlet air temperature (0.91°C.min^{-1}). This quick temperature increase does not occur simultaneously over the whole container's length; it is 13 minutes delayed between the inlet and the middle of the container, 17 minutes between the inlet and the outlet.

A similar behaviour is observed during the heat release period (see Figure 7). After a quick decrease from 45 to 35°C (0.91°C.min^{-1}), an 18 minutes long stable-temperature-period is observed. Then, temperature starts to decrease with a slower rate, meaning the PCM solidification is not complete.

Measured temperatures in the PCM are equal to the inlet temperature 1.5 hours after the temperature change. This means the release of heat is achieved over this period. Therefore, it is obvious the 1 kWh during 2 hours goal is not meet during this experiment.

3.2 Temperature difference measurements

To give an idea of the heating power, it is interesting to study temperature difference measurements during the solidification period (see Figure 8). Although constant temperatures are measured in the material for a while, this is not visible when looking at the temperature difference over the whole heat exchanger. It remains higher than 8°C during the beginning of the experiment (18 minutes approximately), then it decreases rather linearly to 2°C over 50 minutes.

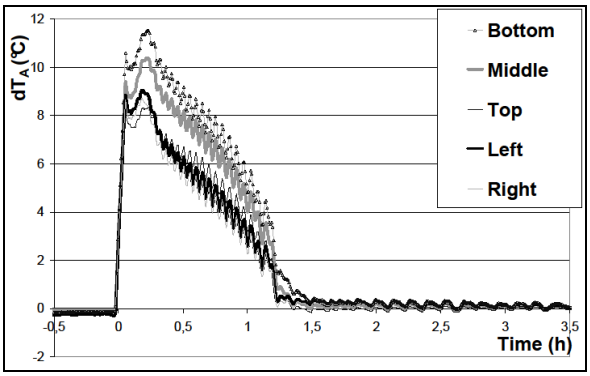

Figure 8: Temperature difference measurement during the solidification period

However, the temperature difference is not homogeneous over the cross-section; an averaged 3°C difference is observed between the different sensors (the standard deviation is 1.2°C). Lower values are measured close to the sidings while the highest temperature differences are measured in the middle of the cross section and at the bottom. However, the standard deviation is lower than 0.1°C when the exchanger is neither storing nor releasing heat. Observed difference could be the consequence of non-uniform velocities over the cross-section. As a consequence, it seems necessary to estimate the airflow rate Q_V accurately to compute the heating power.

3.3 Airflow measurements and comparison with CFD results

The hot-wire anemometer was used to achieve airspeed measurements in the downstream section when the heat exchanger was not installed in the test-section. It is placed 0.1 m away from the end of the downstream section, and moved successively at nine different locations; in the middle of the cross section, close to the position of the temperature sensors, and close to the corners.

Measurements are averaged over 90 seconds and results are presented in Figure 9. Relative coordinates are used to identify the sensor positioning. It is defined on a [-1; 1] range, where x*=0 corresponds to the middle-length, and z*=0 to the middle-height.

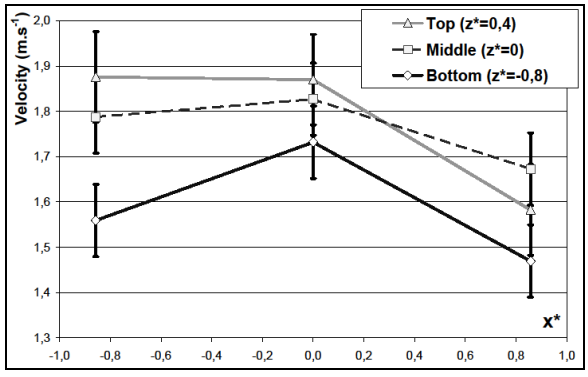

Figure 9: Airspeed measurements achieved in the downstream section

The velocities are rather similar for four locations (z*= [0; 04], x*= [-0.85; 0]). The average value is 1.84 m.s^{-1} and the

standard deviation is 0.04 $m.s^{-1}$. On the other hand, lower values are measured close to the right siding (x*=0.85) and at the bottom of the downstream section (z*=0.8). The average value is 1.6 $m.s^{-1}$ and it drops down to 1.47 $m.s^{-1}$ close to the right corner.

Under a lower airflow rate, a constant heating power results in a higher a temperature difference. This could explain why temperature difference measurements are different from the bottom to other sidings (see Figure 8).

To assess this statement, a commercial CFD software (Computational Fluid Dynamics) is used to simulate the airflow in the whole downstream section. An unstructured mesh is selected and the air volume is meshed with more than 500 000 polyhedral cells. This mesh is refined close to the sidings, so the 0.01 m boundary layer is composed of 10 layers, as presented in Figure 10.

The boundary conditions are:

- An homogeneous 900 $m^3.h^{-1}$ airflow at the inlet;
- A zero-pressure condition at the outlet;
- Wall conditions for other boundaries.

Reynolds number is higher than 35 000, meaning the airflow is turbulent. Therefore, a classical k-epsilon turbulence model is selected. As the main goal is to give a general idea of the airflow properties, no detailed study is achieved on the influence of the simulation parameters.

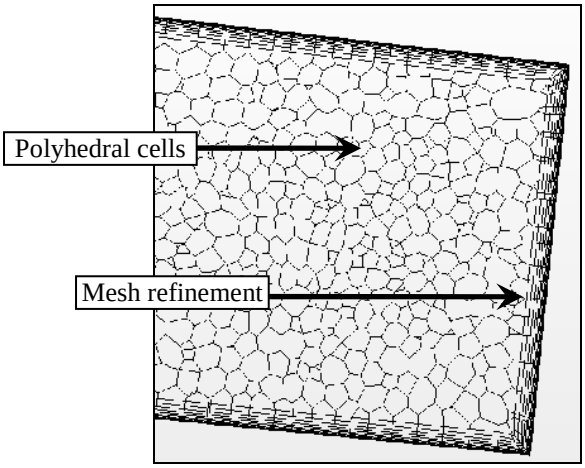

Figure 10: Right part of the meshed cross-section located 0.1 m before the end of the downstream section

Finally, the air velocity is observed in the cross-section located 0.100 m before the heat exchanger (the exchanger is not simulated). Differences are computed using equation (3) and results are presented in Table 4.

Table 4: Velocity differences between simulation results and measurements

	x*= -0.85	x*= 0	x*= 0.85
z* = 0.4	-0.6%	-4.7%	-15.6%
z* = 0	-4.6%	-6.5%	-10.4%
z* = -0.8	-3.8%	-8.9%	-10.3%

$$\Delta U = \frac{U_{Meas} - U_{Sim}}{U_{Sim}} \quad (3)$$

Where: ΔU is the velocity difference (-);
U_{Meas} is the measured velocity ($m.s^{-1}$);
U_{Sim} is the computed velocity ($m.s^{-1}$).

Simulation results are consistently higher than measured velocities (the average difference is 7.3 %). This could results from air leakages, and means the airflow crossing the exchanger is lower than the programmed value. More, differences are not homogenous over the whole cross-section; higher differences are observed on the right side (x*=0.85) than on the left (x*=-0.85), while average differences are observed at middle-length (x*=0). As the simulated geometry is symmetric, so are the numerical results. The computed differences are resulting from the values of U_{Meas}, which are varying from one side to another (6 to 16 %). Considering the measurement uncertainties however, it would be rather risky to take into account these variations in the calculation the heating power.

Therefore, it is better to use a single measurement to estimate the total airflow. It can be quickly estimated with reducing the airflow rate according to the comparison of the velocities as presented in (4).

$$\dot{Q}_V = U_{Meas} \cdot S \cdot \left(1 - \overline{\Delta U}\right) \quad (4)$$

Where: S is the cross-section (m^2);

Finally, the pressure difference across the heat exchanger remains the same during the whole experiment (92.0 ± 1.3 Pa).

3.4 Estimation of the heating power and of the energy released by the system

The heating power P can now be calculated as presented in (1). The temperature difference is the average value of the 5 measurements achieved both in the upstream and in the downstream section as presented in 3.1. The airflow rate is estimated from airspeed measurements as presented in (4). Results are presented in Figure 11.

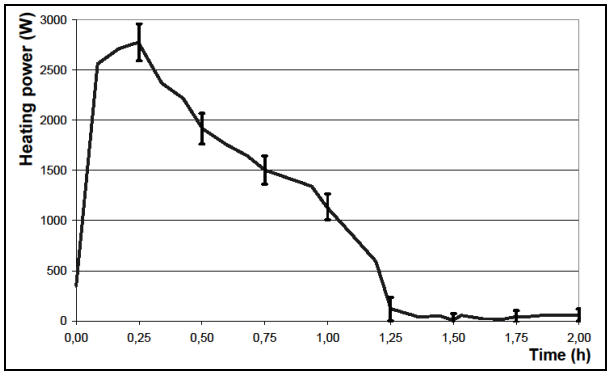

Figure 11: Measured heating power after the temperature change (from 45 to 20°C).

The uncertainty on the measured heat power *u(P)* is estimated with the general equation (5) given in [4].

$$u(P) = \sqrt{\sum \left(\frac{\partial P}{\partial x_i} \cdot \sigma(x_i) \right)^2} \quad (5)$$

Where: x_i is any of the variables used to compute P;
$\sigma(x_i)$ is the standard deviation associated with x_i.

The heating power can be integrated over the heat release period. The result represents the cumulative energy released by the heat exchanger. In this case, the uncertainty can also be estimated with using the same approach as presented in (5). Results are presented in Figure 12.

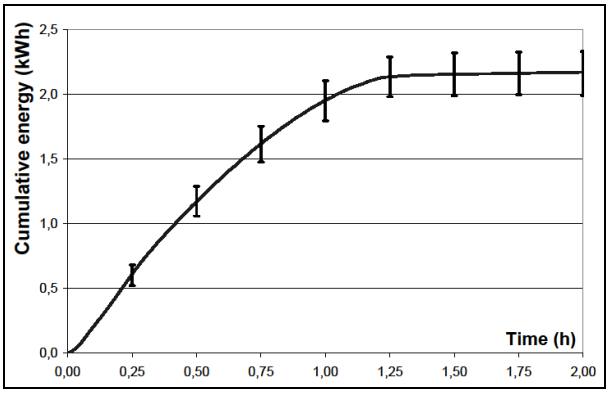

Figure 12: Cumulative energy released by the system after the temperature change (from 45 to 20°C).

As the airflow rate remains constant over the experiment, the heating power follows closely the measured temperature difference. As a consequence, it rises quickly to (2770 ± 180) W for 15 minutes, and then it decreases regularly to (500 ± 120) W in almost 1 hour. The initial goal (obtaining a minimum 1 kW heating power during 2 hours) is no more reached 1 hour after the temperature change.

However, the cumulative energy curve indicates the total energy released from the exchanger is (2.16 ± 0.16) kWh. This means the exchanger has stored enough energy to meet the heating demand.

Moreover, the theoretical value can be estimated by considering the measured properties of PCM (see Table 1) and the general properties of the aluminium (thermal capacity = 897 $J.kg.K^{-1}$, density = 2700 $kg.m^{-3}$). Under a 25 K temperature difference, 2.6 kWh should be stored in the heat exchanger. The relative difference with the experimental value is close to 17 %. This difference can be partially explained as PCM losses are observed during the experiment. This may result from leakages at the sidings of the containers. It was also observed the heat exchanger was not exactly horizontally installed (the slope is close to 0.5 %), which can lead to mass loss through the air vents.

3.5 Outlook

Other tests should be conducted soon to observe the influence of the airflow rate on the heating power. On a theoretical point of view, the cumulative energy should not depend on the airflow rate. Verifying this point would allow concluding on the reliability of both the method and the instrumentation.

Even if stable temperature is observed in the PCM during the solidification period, the heating power decreases regularly during this period. Then, it seems rather hard to obtain a constant heating power under such conditions, and so as to meet the objectives. However, the heat exchanger is designed so enough energy can be released. An alternative could be to consider a variable airflow rate rather than a constant value. To do this, a control device should be implemented in order to get a constant heating power.

4. CONCLUSION

In this paper, a heat exchanger containing more than 27 kg of PCM is presented and tested within an air supply system. It is designed so it can store enough energy to replace a 1 kW heat pump during 2 hours.

The heat exchanger is composed of aluminium containers and combined with cooling fins. The assembly is insulated and special care is taken to limit air leakages and mass losses resulting from density change during the melting of PCM.

The air supply system is equipped with specially designed downstream and upstream sections. It is used to produce a constant airflow rate with temperature changes, selected so the PCM is allowed to melt, then to solidify.

Temperatures measurements achieved within the PCM allowed to observe a stable temperature during the solidification. However, the evolution of the heating power is quite different. Even if the heat exchanger is releasing enough energy, the initial objective could not be met: the heating power reaches as much as (2770 ± 180) W at the beginning of the experiment and is lower than (500 ± 120) W after 90 minutes. Further tests should be conducted under various airflow rates to assess the results presented here. However, it seems hard to meet the actual goal with considering constant airflow rates, so one should focus on controlling the airflow rate.

ACKNOLEDGMENTS

This work has been made with the support of the French ANR project STOCKAIR2.

REFERENCES

[1] Virgone J., Kindinis A. Peak power reduction using a PCM storage coupled with a heat pump in a ventilation system. *Innostock 2012, Lleida, May 2012, 9p.*

[2] Lazaro A., Dolado P., Maran M.J., Zalba B., PCM air heat exchangers for free cooling application in buildings: Experimental results of two real-scale prototypes, Energy Conversion and Management 50 (3) 2009, p. 439-443

[3] Arzamendia Lopez J .P., Kuznik F., Baillis D., Virgone J., Numerical modelling and experimental validation of a PCM to air heat exchanger, Energy and Buildings 2013, submitted.

[4] EURACHEM/CITAC. Quantifier les incertitudes dans les mesures analytiques, 2nd Ed., France. SLR Ellison (LGC-UK) – M ROSSLEIN (EMPA- Switerland) – A WILLIAMS (UK), 2000.